PROCEEDINGS A

royalsocietypublishing.org/journal/rspa

Research

Cite this article: Punacha S, Berg S, Sebastian A, Krinski VI, Luther S, Shajahan TK. 2019 Spiral wave unpinning facilitated by wave emitting sites in cardiac monolayers. *Proc. R. Soc. A* **475**: 20190420.
http://dx.doi.org/10.1098/rspa.2019.0420

Received: 4 July 2019
Accepted: 23 September 2019

Subject Areas:
biophysics, medical physics

Keywords:
excitable media, spiral waves, unpinning window, cardiac arrhythmia

Authors for correspondence:
T. K. Shajahan
e-mail: shajahan@nitk.edu.in
Stefan Luther
e-mail: stefan.luther@ds.mpg.de

Electronic supplementary material is available online at https://doi.org/10.6084/m9.figshare.c.4686101.

THE ROYAL SOCIETY PUBLISHING

Spiral wave unpinning facilitated by wave emitting sites in cardiac monolayers

Shreyas Punacha[1], Sebastian Berg[2], Anupama Sebastian[1], Valentin I. Krinski[2], Stefan Luther[2] and T. K. Shajahan[1,2]

[1]National Institute of Technology Karnataka, Surathkal, Mangalore 575025, India
[2]Max Planck Institute of Dynamics and Self Organization, Göttingen 37017, Germany

SP, 0000-0002-4523-9627

Rotating spiral waves of electrical activity in the heart can anchor to unexcitable tissue (an obstacle) and become stable pinned waves. A pinned rotating wave can be unpinned either by a local electrical stimulus applied close to the spiral core, or by an electric field pulse that excites the core of a pinned wave independently of its localization. The wave will be unpinned only when the pulse is delivered inside a narrow time interval called the unpinning window (UW) of the spiral. In experiments with cardiac monolayers, we found that other obstacles situated near the pinning centre of the spiral can facilitate unpinning. In numerical simulations, we found increasing or decreasing of the UW depending on the location, orientation and distance between the pinning centre and an obstacle. Our study indicates that multiple obstacles could contribute to unpinning in experiments with intact hearts.

1. Introduction

In many physiological systems, a wave of excitation coordinates functioning of millions of cells that constitute the system. The excitation is produced locally within each cell, hence as long as the cells are excitable the wave can travel without any attenuation. Waves of this type are found in a variety of systems, including in chemical reactions [1], social amoebae [2] and in physiological tissue such as brain [3], heart [4], retina [5] and uterus [6].

Two important properties of these waves are: (1) the conduction velocity of excitation waves depends on the curvature of the wave, i.e. convex waves travel slower than plane waves whereas concave waves travel faster than plane waves. (2) After excitation, the tissue remains inactive for a characteristic period called the refractory time. Because of these properties of the propagation, excitation waves can form a spiral shape and rotate indefinitely in the supporting medium [7]. Such rotating waves are often associated with functional disorders in physiological tissue, like reentrant electrical activity in the heart during cardiac arrhythmias [8]. Hence, it is important to devise methods to eliminate them. But rotating waves in heterogeneous excitable media tend to attach to heterogeneities and form stable pinned waves [4,9,10]. These pinned waves have to be unpinned first to be able to eliminate them. They can be unpinned if an electric stimulus is delivered very close to the pinning centre and within a specific time interval called the unpinning window (UW), i.e. the stimulus has to be within a narrow spatial and temporal window [11–13].

The problem of spatial location can be solved by using electric field pulses, which can generate secondary excitations from heterogeneities in the tissue [13,14]. Since these excitations are generated from possible pinning centres, they can appear close to the core of the spiral. But they still have to be generated within the UW of the wave. Recently, many groups have started using periodic field pulses to increase the chances of unpinning and these are found to be very effective in LEAP [15,16]. Studies so far have focused on unpinning a rotating wave by secondary excitations emanating from the pinning centre itself (except a very recent paper by Tom Wörden *et al.*, which studied control of multiple pinned spirals in an excitable media [17]). However, these studies show that unpinning window is quite narrow compared to the experimental studies in intact heart [16,18]. This induced us to study the role of multiple wave emitting sites (WES) in the unpinning process. Also, multiple heterogeneities in close vicinity offer the possibility of additional stimulus sites and additional anchoring sites. In such cases one need to examine how the distribution of heterogeneities modifies the UW. Despite their critical importance in low-energy antifibrillation techniques, this problem has not received much attention so far. We study how these additional obstacles can alter the unpinning of a single spiral.

In this paper, we show that secondary excitations emanating from nearby heterogeneities can unpin a wave attached in the vicinity in monolayers of cardiac cells. We then undertake a detailed numerical study of the wave unpinning in the presence of two heterogeneities. We found that the UW either increases or decreases in the presence of additional heterogeneity. Their influence depends on their orientation with respect to the electric field, distance from the obstacle and the size. Along certain orientations unpinning completely fails.

2. Methods

(a) Experiments

The experiments were conducted in a monolayer of cardiac myocytes extracted from chicken embryos, prepared as described in [19,20] and plated as circular disks of 10 mm diameter. A hole with 2 mm diameter was drilled in the middle of the glass plate, creating a central heterogeneity without any cells. Rotating waves were initiated in the monolayer by high-frequency field pacing. The excitation of the cardiac myocytes was tracked using a calcium-sensitive dye (Calcium Green, Invitrogen) and the resulting calcium waves were mapped with an Olympus MVX10 microscope and a Photometrics Cascade 512 EMCCD camera. Custom written softwares were used for data acquisition and further analysis.

During the experiment, the fluorescent signal was averaged over a small user-selected area and then it was smoothed using a band pass filter. When this fluorescent activity from the pre-selected area of the monolayer exceeded a certain threshold, we applied electric field pulses at chosen phases of the rotating wave. The strength of the field varied from $1\,\mathrm{V\,cm^{-1}}$ to $5\,\mathrm{V\,cm^{-1}}$ and its frequency from 0.6 to 2.0 Hz, and each stimulus lasted for 20 ms.

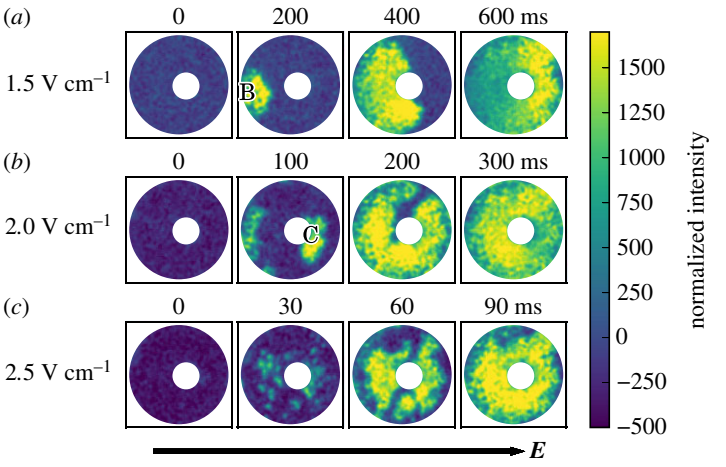

Figure 1. An electric field pulse initiates multiple wave emitting sites in a cardiac cells monolayer. The electric field $\boldsymbol{E}$ is applied from left to right at $t = 0$ s. (*a*) At $\boldsymbol{E} = 1.5$ V cm^{-1}, waves are emitted only from the monolayer outer boundary (B), see $t =$ 200 ms. (*b*) At $\boldsymbol{E} = 2$ V cm^{-1}, the outer monolayer boundary (B) and the obstacle at the centre (C) are emitting waves. (*c*) At 2.5 V cm^{-1}, excitation can also originate from smaller heterogeneities in the monolayer. Note that full excitation occurs much earlier in (*c*). (Online version in colour.)

(b) Mathematical model

We use the Fitzhugh Nagumo model (FHN) to simulate the spiral wave in a two-dimensional medium. The model equations are as follows:

$$\frac{\partial u}{\partial t} = \frac{1}{\epsilon}(u(1-u)(u-a) - v) + D\nabla^2 u \tag{2.1}$$

and

$$\frac{\partial v}{\partial t} = bu - v, \tag{2.2}$$

where u and v stands for transmembrane voltage and gating variable, respectively. The parameter values are chosen as $a = 0.085$, $b = 0.25$ and $\epsilon = 0.045$. The space and time coordinates are discretized for a spatial step of $\Delta x = \Delta y = 0.1$ and time step of $\Delta t = 0.0001$. We use a square domain of grid size 300×300. For presentation purpose, we postulate the time units to 20 ms and space units to 1 mm. That is, 1 time step is equivalent to 0.002 ms and 1 grid space is equivalent to (1/10) mm. The diffusion coefficient D is set to 1 cm^2 s^{-1}. With this choice of spatial and temporal scales the wavelength and conduction velocity approximately match with those observed in the experiments. These equations are solved using explicit forward Euler method in time and the five point finite difference method in space. The accuracy of the Euler scheme has been tested systematically for smaller spacial resolutions ($dx = 0.05, 0.01$) and the quantities such as action potential duration and wavelength of the spiral are found to agree with each other.

The no flux boundary condition with an applied field E is given by,

$$\hat{y} \cdot (D\nabla u - \boldsymbol{E}) = 0, \tag{2.3}$$

where $\hat{y}$ represents the unit vector along the direction of applied electric field $\boldsymbol{E}$ (V cm^{-1}). The boundary conditions are imposed on the obstacle boundary by the phase field method [21]. The phase field (ϕ) modifies equation (2.1) to:

$$\frac{\partial u}{\partial t} = \frac{1}{\epsilon}(u(1-u)(u-a) - v) + \nabla \cdot (D\nabla u) + \nabla \ln \phi \cdot (D\nabla u) - \nabla \ln \phi \cdot \boldsymbol{E}. \tag{2.4}$$

A spiral wave rotating in a clockwise direction is initiated in the medium. The wavelength of the spiral is $\lambda = 3.5$ mm. It takes 328 ms to complete one free rotation around an obstacle of

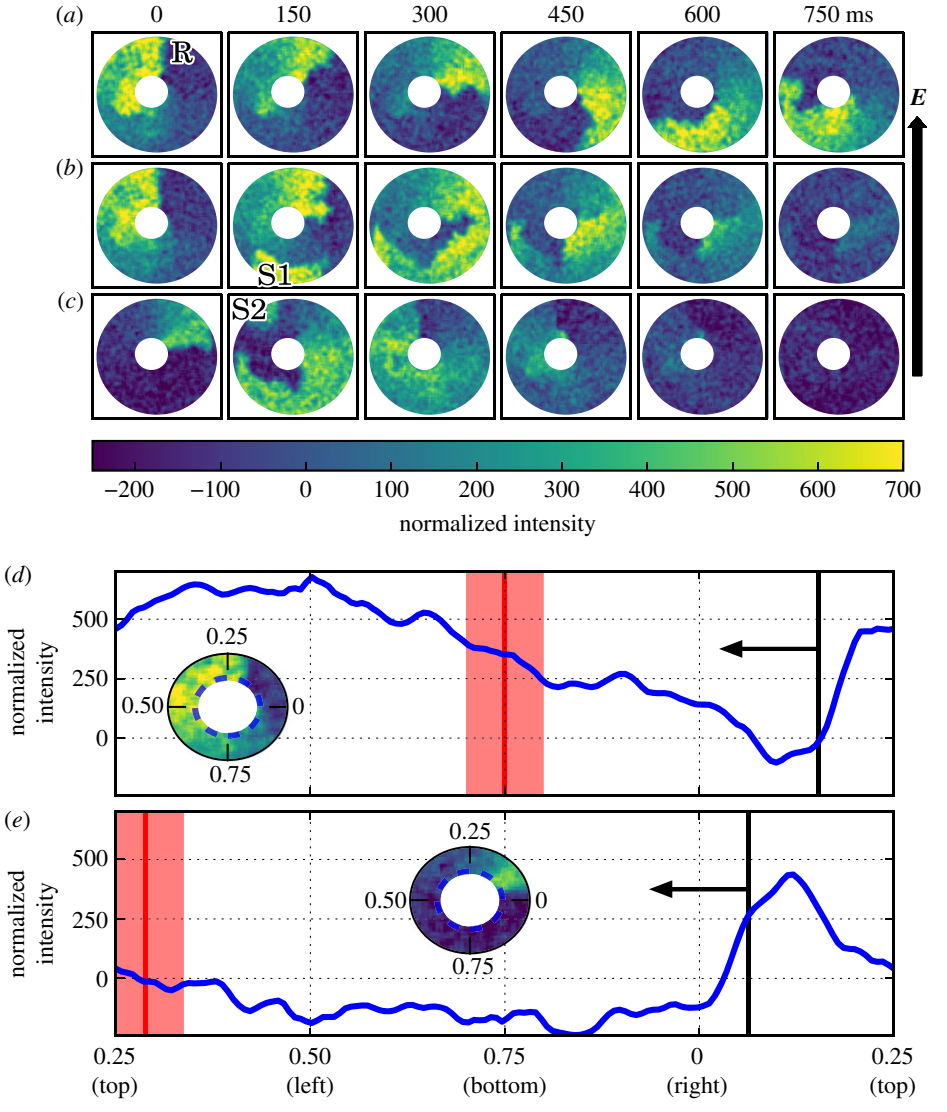

Figure 2. Unpinning by two-wave emitting sites in a cardiac cells monolayer. (*a*) A rotating wave R pinned to the obstacle. (*b*) A field stimulus is given from bottom to top ($t = 0$). Wave emitted from the lower boundary (S1) moves opposite to the wave R. This would eventually collide and annihilate the wave R. (*c*) The stimulus is applied when the wave R is slightly more advanced. A second site (S2) from top boundary also gets excited by the stimulus ($t = 150$ ms), which terminates the rotating wave R. (*d*,*e*) The rotating wave R along the circumference of the obstacle at the time of stimulus, corresponding to the images in (*b*) and (*c*), respectively. The wide vertical red line indicates the location of the wave emission site (S1 or S2), and black vertical line with a leftward arrow indicates the location of the wavefront. The insets show the fluorescent activity directly around the heterogeneity indicating the corresponding phase. (Online version in colour.)

radius 3 mm located at the centre. Far-field pacing (FFP) shock of duration 0.8 ms is applied in a horizontal direction with a weak electric field of strength $E_0 = 1.2\,\mathrm{V\,cm^{-1}}$. The electric field gives rise to secondary excitations that can potentially unpin the spiral. The phase of the spiral at the time of the stimulus is an important parameter which determines the UW [22].

The phase here is the location of the wavefront of the pinned spiral at the time of the stimulus with the zero of phase being the place of wave emission from the heterogeneity. The phases of the stimuli that leads to successful unpinning is the UW.

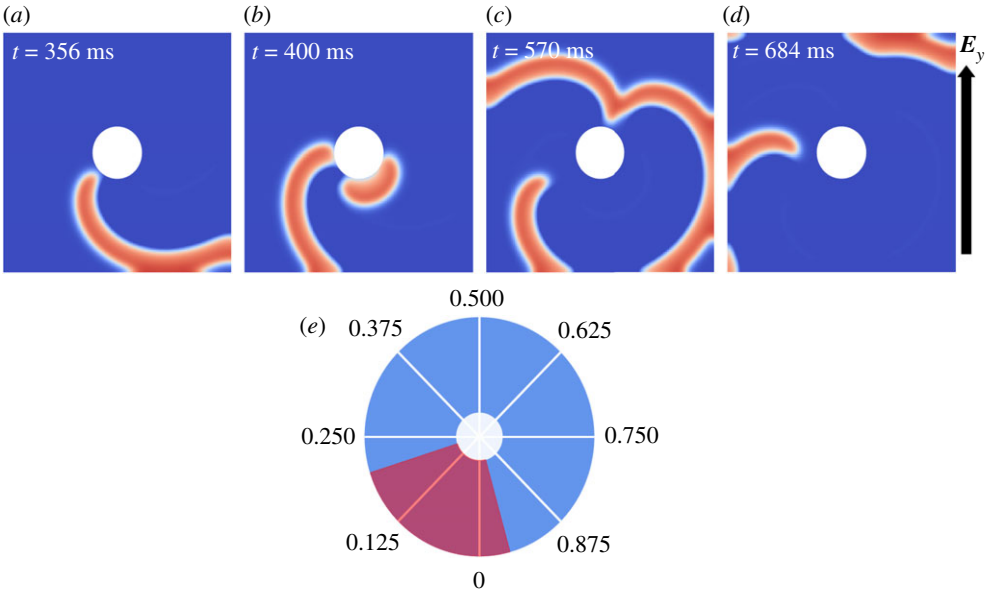

Figure 3. Numerical simulations showing successful unpinning by FFP for a single obstacle. (*a*) A rotating spiral is pinned to an obstacle of radius 3 mm located at the centre of the domain. (*b*) Nucleation of secondary excitation from the obstacle when a pulsed stimulus is applied in a vertical direction as indicated by the black arrow on the right. (*c*,*d*) Detachment of pinned spiral from the obstacle. (*e*) Unpinning window of single obstacle: Each angle inside the circle corresponds to the phase of the pinned spiral at the time of the stimulus. It is measured with respect to the point of secondary excitation represented by '0' in the figure. Red shaded sector indicates the unpinning window. All the simulations are done using Fitzhugh Nagumo model. (Online version in colour.)

In order to study the effect of additional WES on the wave unpinning, we introduced a second obstacle. We considered the unpinning to be successful only if the spiral drifted away from both the obstacles at the end of one period of the spiral.

3. Experimental results

Field stimulus induces WES from boundaries of heterogeneities. In our experiments there were two major boundaries: the concave boundary of the entire monolayer and the convex boundary of the circular hole within the monolayer.

Figure 1 shows wave emission from these boundaries as we increase the field strength. When the field strength is low ($1.5\,\mathrm{V\,cm^{-1}}$) only the concave outer boundary of the monolayer is excited. But at $E = 2\,\mathrm{V\,cm^{-1}}$ both the outer monolayer boundary and the central obstacle boundaries are excited. At higher field ($E = 2.5\,\mathrm{V\,cm^{-1}}$) wave emission is observed even from small-scale heterogeneities such as non-excitable cells like fibroblasts and fluctuations in cell to cell connectivity, as predicted by previous theoretical studies [23–25]. An attached wave can be unpinned by any of these excitations.

However, if the medium is already excited, only some of the wave emission sites will be active during a stimulus. For example, consider the monolayer in figure 2*a*, where an attached wave is rotating clockwise. When we apply an electric field ($\approx 3\,\mathrm{V\,cm^{-1}}$) directed vertically upwards, there can be wave emission from the lower boundary (S1, figure 2*b*) and the upper boundary (S2, figure 2*c*). But at the time of the stimulus, if any of these locations are refractory due to the passing of the rotating wave, those sites will not emit secondary excitation.

There is a short time window after the wave, such that secondary excitations in that window propagate only in the direction opposite to the rotating wave [26]. This is the UW. A stimulus

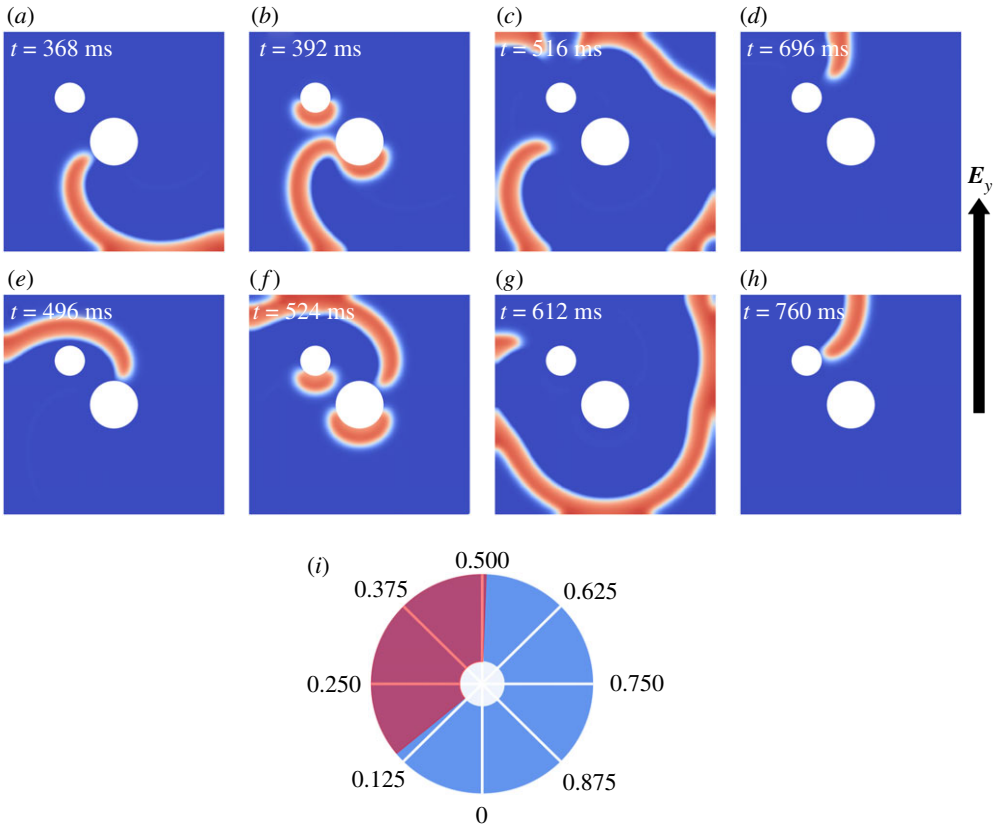

Figure 4. Success and failure of unpinning of spiral pinned to an obstacle in the presence of the additional wave emitting site: black vertical arrow on the right indicates the direction of applied electric field of strength $E_0 = 1.2$ V cm^{-1}. (*a*) Spiral is pinned to an obstacle of radius 3 mm with second obstacle of radius 2 mm nearby. (*b*) Nucleation of secondary excitation by the application of short timed pulse. (*c*,*d*) Detachment of the original spiral from the obstacle resulting in successful unpinning. (*e*) Spiral wave pinned to the central obstacle at a different phase. (*h*) The spiral getting pinned back to the second obstacle leading to failure of unpinning. (*i*) The unpinning window for the above configuration of the obstacles. (Online version in colour.)

within the UW can unpin an attached wave. Thus, if either S1 or S2 gets activated in the UW of the rotating wave, the wave will be unpinned.

In figure 2*b*, the stimulus was applied when the wave is at the 12H location on the obstacle. The site S2 happened to be in the refractory tail of the wave, and S1 was activated within the UW of the rotating wave, and the wave got unpinned. Another stimulus when the wavefront was at 3H (figure 2*c*) excited both S1 and S2. Here, S1 was fully excitable and could propagate both directions, but S2 was within the UW and eliminated the rotating wave. Thus the UW enlarges when there are two WES. Which of them participates in the unpinning event depends on the location of the rotating wave at the time of the stimulus.

4. Numerical results

Numerical simulations are carried out to reveal the mechanisms underlying complex interaction of excitable waves with obstacles and their effect on the UW. In cardiac monolayers, the boundary of the monolayer acted as an additional WES. In the following section, we systematically study the effect of additional WES by introducing another obstacle near the pinning centre.

In the following section, we systematically scrutinize the conditions for success and failure of unpinning by introducing an additional WES near the spiral core. Figure 3 shows the unpinning

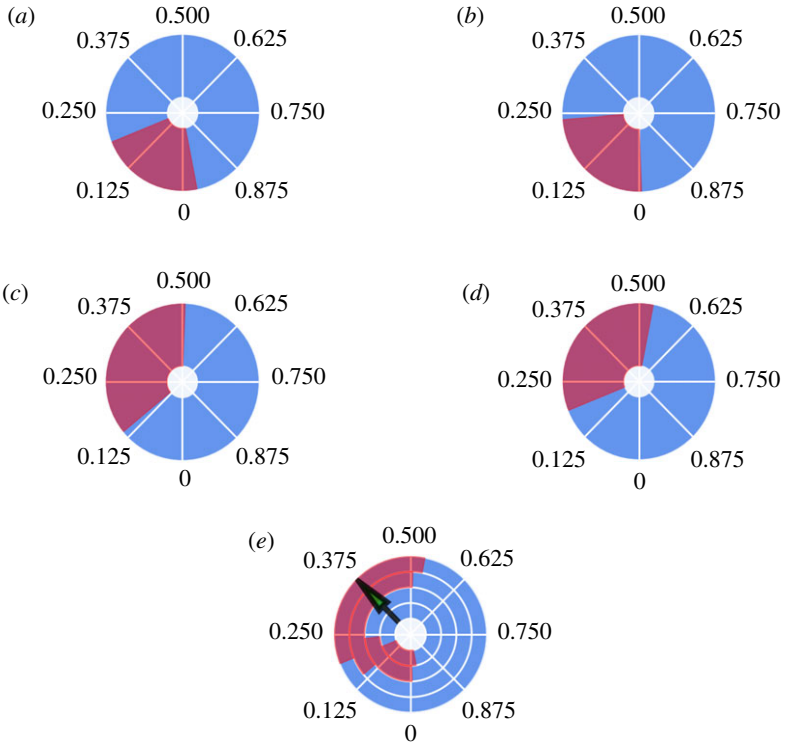

Figure 5. Unpinning window for different distances of additional wave emitting site around the central obstacle: The orientation of the additional wave emitting site is as shown in figure 4. By keeping the radius of both obstacles fixed, we change the distance of the second obstacle from the first. The red shaded sectors in subplots (*a–d*) indicates the unpinning window for the distance between the obstacles 5.656, 7.707, 8.484 and 9.898 mm, respectively. Subplot (*e*) summarizes figure (*a–d*). The white shaded circular region at the centre of the obstacle indicates the central obstacle. The arrow indicates the orientation of the second obstacle. Each white concentric circle denotes the distance of the second obstacle from the central obstacle. The red shaded region corresponds to the unpinning window for a fixed distance between the two obstacles. (Online version in colour.)

of the spiral due to the secondary wave emitted from the single obstacle. We find the continuous phase window that leads to unpinning of the spiral to be 0.24.

To estimate the effect of second WES on the UW, we introduce a new obstacle of 2 mm radius (figure 4). A global electric field now creates two excitable waves, one form each of the obstacle. Depending on the time at which the pulse is given, the spiral can (a) successfully unpin from the obstacle (figure 4*d*) (b) detach but repin back to the second obstacle (figure 4*g*,*h*) or (c) reattach to the first obstacle at a different phase. For the choice of orientation of the obstacle considered in figure 4 the UW is found to be 0.36, which is 50% more than that of the single obstacle UW (figure 3*b*).

For a given orientation of the obstacle and fixed strength of the electric pulse, the width of the UW critically depends on the distance of the second obstacle from the first. If the distance is very small, like in figure 5*a* the UW shrinks to 0.21 but widens significantly for larger distances. The variation of the UW with distance is summarized in figure 5*e*. The reason for the shrinking of the UW at smaller distances is because of the obstacles acting as a single entity when they are very close to each other. Owing to this merging of the obstacles, the spiral is able to sustain its pinned rotation.

Interestingly, the increase in the width of the UW does not carry over uniformly across all the locations of the additional wave emitting site. To study the dependence, we place the second obstacle at eight different orientation around the central obstacle, each time shifting it by an angle of 45° (0.125 phase units) as shown in figure 6. For majority of orientations, the UW either

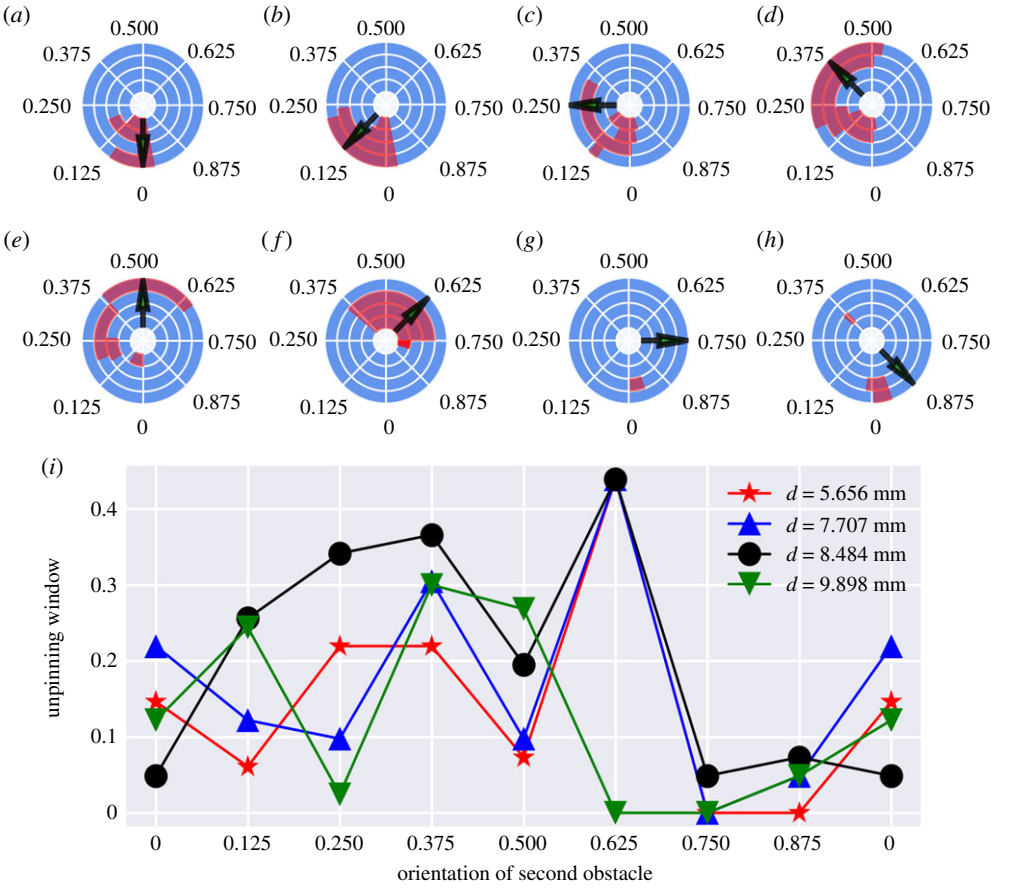

Figure 6. Unpinning window for different orientation of additional wave emitting site around the central heterogeneity: the shaded circular region at the centre of the figure represents the obstacle. The arrow indicates the angle at which the second obstacle is located. By keeping the radius of both the obstacle fixed, we change the distance of the second obstacle from the first. Each white concentric circle denotes the distance of the second obstacle from the central obstacle. The red shaded region corresponds to the unpinning window for a fixed distance between the two obstacles. Figure (*a–h*) represents unpinning window of 8 different orientation of the additional wave emitting site having a radius of 2 mm around the central heterogeneity. The distances between the first and second obstacles are fixed to 5.656, 7.707, 8.484 and 9.898 mm, respectively. (*i*) Plot of orientation of the second obstacle *versus* the unpinning window for different distances between the obstacles. (Online version in colour.)

shrieked or vanished entirely for very small distances. From figure 6*i*, we can infer the qualitative behaviour of the UW for different orientations and distances of the additional WES.

Then, we comprehensively study the effect of variation of the size of the second obstacle on the UW. We systematically vary the radius of the second obstacle to be 1.5 mm (electronic supplementary material, figure S1), 2.0 mm (figure 6) and 2.5 mm (electronic supplementary material, figure S2). As the size of second obstacle increases, the boundary separation between the obstacles becomes negligible. With this setting, both the central and second obstacle acts like a single entity since the excitation is unable to propagate between them (Conduction Block) [27]. This increases the chances of spiral repinning to the second obstacle and hence significantly reduces the UW.

Figure 7 indicates the dependence of the UW on the orientation of second obstacle for three different sizes of the obstacle. Here, each subplot represents the UW for distance 5.656, 7.707, 8.484 and 9.898 mm, respectively. For a fixed distance between the obstacles, the UW either vanishes or is very low for most of the orientations when the obstacle size is large. Unpinning will be

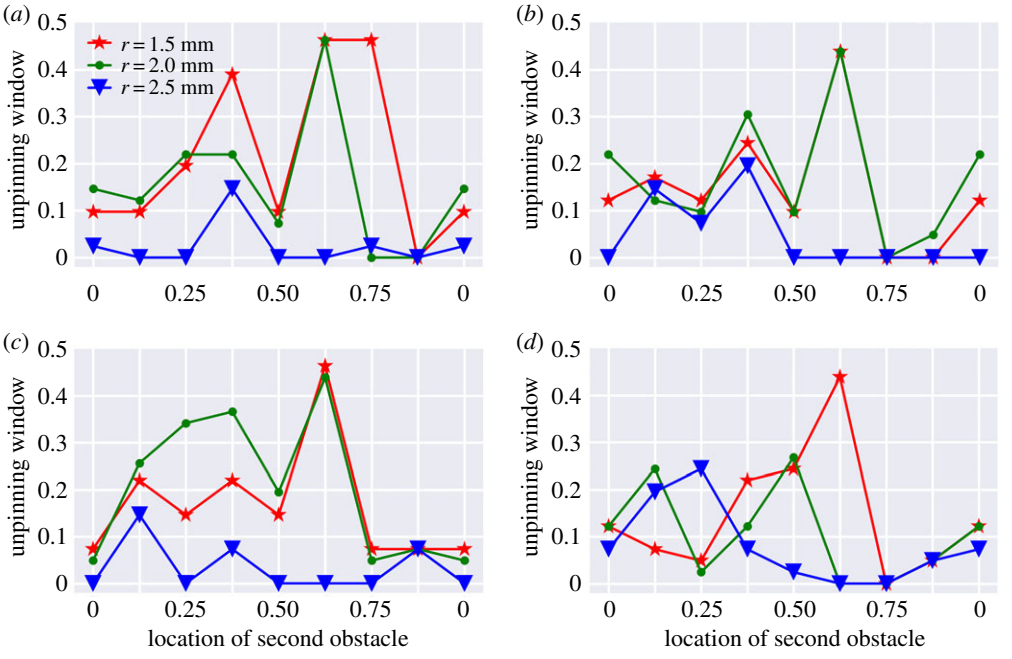

Figure 7. Dependence of unpinning window with the location of second obstacle: Figure (*a–d*) represents the unpinning window plotted for four different distances 5.656, 7.707, 8.484 and 9.898 mm between the centres of obstacles. Eight different location of the second obstacle varying by an angle of 45° is taken over *x* axis (as clock positions) and corresponding unpinning window is plotted. Inside each figure, the unpinning window for three different radii of the second obstacle (denoted by 'r') corresponding to 1.5, 2 and 2.5 mm are shown. (Online version in colour.)

easier if the additional WES is small. This is because smaller obstacles reduce the chances of spiral repinning to the obstacle. This explains the large UW for smaller-sized obstacles shown in figure 7.

5. Discussion

In this paper, we study how the introduction of an additional WES modifies the UW of a pinned spiral wave. In the experiments using cardiac monolayers we found that a wave pinned to an obstacle can be unpinned by a secondary wave initiated from another nearby obstacle. We then systematically investigated unpinning in the presence of two heterogeneities and found that the second obstacle can significantly alter the UW of a pinned spiral wave. The UW alter depending on the details of how the second obstacle is placed with respect to the pinning centre.

Our experiments show that a higher number of WES can be recruited in a heterogeneous medium simply by increasing the strength of the applied electric field. Extra obstacles in the proximity act as extra WES which can help in unpinning but they can also act as a additional pinning sites. We have chosen the size of the secondary obstacle so that it is possible to have stable pinned spirals (that is, the diameter is more than the spiral core). Such large obstacles are also are more likely to acts as virtual electrodes than smaller obstacles, for the field strengths we use.

We observed widening of the UW for certain orientations and distances of additional WES. UW is seen to decrease or sometimes vanish altogether for smaller distances due to repinning. Unpinning fails if the separation between the obstacle boundary is too small compared to the wavelength of the spiral. This is due to the obstacles acting like a single entity and the wave is unable to propagate between them. We also observe that unpinning success rate decreases for a configuration containing a large secondary obstacle than that of a small one, as large obstacle can contribute to maximum probability of repinning.

Though these studies are conducted in a two-dimensional model, the phenomenon such as pinning, unpinning and secondary excitations described in the paper were observed in previous detailed studies carried out on ionic models such as Luo-Rudy I [23] and Beeler Reuter [28]. Hence, we expect the qualitative features of our study to be valid even in realistic ionic models. However, the quantitative details such as the width of the UW are model dependent.

Studies of unpinning using two-dimensional experimental and numerical models show that the UW in such cases are very narrow [16,18]. However, multiple field pulses are much more efficient in *in vivo* experiments. We suspect several factors, including multiple heterogeneities, and three-dimensional structure of the heart could be assisting the unpinning. Our study using two obstacles point in this direction. Further investigations are required to understand how multiple waves finally alter the unpinning.

Data accessibility. A movie version of spiral wave unpinning in case of two obstacles along with raw data, python scripts and figures corresponding to additional wave emitting site having radius of 1.5 and 2.5 mm are available as electronic supplementary material. All the data supporting the findings of this study are available at https://doi.org/10.5281/zenodo.3456886.

Authors' contributions. S.P. designed the numerical study, carried out simulations and wrote the paper. S.B. designed the experimental data analysis software, carried out experimental data analysis and took part in numerical study. A.S. carried out systematic simulations. V.I.K. conceived the experiments, carried out analysis and wrote the manuscript. S.L. devised the experimental study and coordinated the whole study. T.K.S. designed the experimental and numerical study, carried out cell culture experiments and data analysis, conceived and designed numerical study and wrote the manuscript.

Competing interests. The authors declare that they have no competing interests.

Funding. The research leading to the results has received funding from Max Planck Gesellschaft, the European Community Seventh Framework Programme FP7/2007-2013 under Grant Agreement 17 no. HEALTH-F2-2009-241526, EUTrigTreat (S.B., V.I.K. and S.L.). We also acknowledge support from the German Federal Ministry of Education and Research (BMBF) (project FKZ 031A147, GO-Bio), the German Research Foundation (DFG) (Collaborative Research Centres SFB 1002 Project C3 and SFB 937 Project A18), the German Center for Cardiovascular Research (DZHK e.V.) (S.B., V.I.K. and S.L.). T.K.S. thanks SERB (DST) for funding via early career research grant (ECR/2016/000983).

Acknowledgements. We thank Dr M. P. Gururajan, IITB for discussions and insights that greatly assisted our research. We also thank Tariq Baig, Daniel Hornung and Ulrich Parlitz for discussion and Marion Kunze for technical assistance.

References

1. Jahnke W, Skaggs W, Winfree AT. 1989 Chemical vortex dynamics in the Belousov-Zhabotinskii reaction and in the two-variable Oregonator model. *J. Phys. Chem.* **93**, 740–749. (doi:10.1021/j100339a047)
2. Gregor T, Fujimoto K, Masaki N, Sawai S. 2010 The onset of collective behavior in social amoebae. *Science* **328**, 1021–1025. (doi:10.1126/science.1183415)
3. Huang X, Troy WC, Yang Q, Ma H, Laing CR, Schiff SJ, Wu JY. 2004 Spiral waves in disinhibited mammalian neocortex. *J. Neurosci.* **24**, 9897–9902. (doi:10.1523/JNEUROSCI.2705-04.2004)
4. Davidenko JM, Pertsov AV, Salomonsz R, Baxter W, Jalife J. 1992 Stationary and drifting spiral waves of excitation in isolated cardiac muscle. *Nature* **355**, 349–351. (doi:10.1038/355349a0)
5. Yu Y *et al.* 2012 Reentrant spiral waves of spreading depression cause macular degeneration in hypoglycemic chicken retina. *Proc. Natl Acad. Sci. USA* **109**, 2585–2589. (doi:10.1073/pnas.1121111109)
6. Singh R, Xu J, Garnier NG, Pumir A, Sinha S. 2012 Self-organized transition to coherent activity in disordered media. *Phys. Rev. Lett.* **108**, 068102. (doi:10.1103/PhysRevLett.108.068102)
7. Karma A. 2013 Physics of cardiac arrhythmogenesis. *Annu. Rev. Condens. Matter Phys.* **4**, 313–337. (doi:10.1146/annurev-conmatphys-020911-125112)
8. Tung R, Zimetbaum P, Josephson ME. 2008 A critical appraisal of implantable cardioverter-defibrillator therapy for the prevention of sudden cardiac death. *J. Am. Coll. Cardiol.* **52**, 1111–1121. (doi:10.1016/j.jacc.2008.05.058)

9. Valderrábano M, Lee MH, Ohara T, Lai AC, Fishbein MC, Lin SF, Karagueuzian HS, Chen PS. 2001 Dynamics of intramural and transmural reentry during ventricular fibrillation in isolated swine ventricles. *Circ. Res.* **88**, 839–848. (doi:10.1161/hh0801.089259)
10. Bub G, Shrier A, Glass L. 2002 Spiral wave generation in heterogeneous excitable media. *Phys. Rev. Lett.* **88**, 058101. (doi:10.1103/PhysRevLett.88.058101)
11. Takagi S, Pumir A, Pazo D, Efimov I, Nikolski V, Krinsky V. 2004 Unpinning and removal of a rotating wave in cardiac muscle. *Phys. Rev. Lett.* **93**, 058101. (doi:10.1103/PhysRevLett.93.058101)
12. Hörning M, Isomura A, Agladze K, Yoshikawa K. 2009 Liberation of a pinned spiral wave by a single stimulus in excitable media. *Phys. Rev. E* **79**, 026218. (doi:10.1103/PhysRevE.79.026218)
13. Bittihn P, Squires A, Luther G, Bodenschatz E, Krinsky V, Parlitz U, Luther S. 2010 Phase-resolved analysis of the susceptibility of pinned spiral waves to far-field pacing in a two-dimensional model of excitable media. *Phil. Trans. R. Soc. A* **368**, 2221–2236. (doi:10.1098/rsta.2010.0038)
14. Krinsky V, Plaza F, Voignier V. 1995 Quenching a rotating vortex in an excitable medium. *Phys. Rev. E* **52**, 2458–2462. (doi:10.1103/PhysRevE.52.2458)
15. Li W, Ripplinger CM, Lou Q, Efimov IR. 2009 Multiple monophasic shocks improve electrotherapy of ventricular tachycardia in a rabbit model of chronic infarction. *Heart Rhythm* **6**, 1020–1027. (doi:10.1016/j.hrthm.2009.03.015)
16. Luther S *et al.* 2011 Low-energy control of electrical turbulence in the heart. *Nature* **475**, 235–239. (doi:10.1038/nature10216)
17. tom Wörden H, Parlitz U, Luther S. 2019 Simultaneous unpinning of multiple vortices in two-dimensional excitable media. *Phys. Rev. E* **99**, 042216. (doi:10.1103/PhysRevE.99.042216)
18. Shajahan T, Berg S, Luther S, Krinski V, Bittihn P. 2016 Scanning and resetting the phase of a pinned spiral wave using periodic far field pulses. *New J. Phys.* **18**, 043012. (doi:10.1088/1367-2630/18/4/043012)
19. Borek B, Shajahan T, Gabriels J, Hodge A, Glass L, Shrier A. 2012 Pacemaker interactions induce reentrant wave dynamics in engineered cardiac culture. *Chaos* **22**, 033132. (doi:10.1063/1.4747709)
20. Schlemmer A, Berg S, Shajahan T, Luther S, Parlitz U. 2015 Entropy rate maps of complex excitable dynamics in cardiac monolayers. *Entropy* **17**, 950–967. (doi:10.3390/e17030950)
21. Fenton FH, Cherry EM, Karma A, Rappel WJ. 2005 Modeling wave propagation in realistic heart geometries using the phase-field method. *Chaos* **15**, 013502. (doi:10.1063/1.1840311)
22. Behrend A, Bittihn P, Luther S. 2010 Predicting unpinning success rates for a pinned spiral in an excitable medium. In *2010 Computing in Cardiology, Belfast, UK, 26–29 September*, pp. 345–348. Piscataway, NJ: IEEE.
23. Pumir A, Krinsky V. 1999 Unpinning of a rotating wave in cardiac muscle by an electric field. *J. Theor. Biol.* **199**, 311–319. (doi:10.1006/jtbi.1999.0957)
24. Hörning M, Takagi S, Yoshikawa K. 2012 Controlling activation site density by low-energy far-field stimulation in cardiac tissue. *Phys. Rev. E* **85**, 061906. (doi:10.1103/PhysRevE.85.061906)
25. Bittihn P, Hörning M, Luther S. 2012 Negative curvature boundaries as wave emitting sites for the control of biological excitable media. *Phys. Rev. Lett.* **109**, 118106. (doi:10.1103/PhysRevLett.109.118106)
26. Nomura T, Glass L. 1996 Entrainment and termination of reentrant wave propagation in a periodically stimulated ring of excitable media. *Phys. Rev. E* **53**, 6353–6360. (doi:10.1103/PhysRevE.53.6353)
27. ten Tusscher KH, Panfilov AV. 2005 Wave propagation in excitable media with randomly distributed obstacles. *Multiscale Model. Simul.* **3**, 265–282. (doi:10.1137/030602654)
28. Pumir A, Sinha S, Sridhar S, Argentina M, Hörning M, Filippi S, Cherubini C, Luther S, Krinsky V. 2010 Wave-train-induced termination of weakly anchored vortices in excitable media. *Phys. Rev. E* **81**, 010901. (doi:10.1103/PhysRevE.81.010901)